SF2A 2024
M. Béthermin, K. Baillié, N. Lagarde, J. Malzac, R.-M. Ouazzani, J. Richard, O. Venot, A. Siebert (eds)

ULTRA-HIGH-ENERGY COUNTERPARTS OF H.E.S.S. PULSAR-POWERED SOURCES AND MODELING PULSAR HALOS WITH GAMMAPY

K. Sabri[1], Y. A. Gallant[1] and J. Devin[1]

Abstract. The recently published 1LHAASO catalog includes several sources coincident with energetic pulsars. We searched for associations between energetic pulsars and LHAASO's Kilometer Squared Array (KM2A) sources, and found 6 KM2A counterparts of firmly identified or highly rated candidate H.E.S.S. pulsar wind nebulae. Given the age of these sources, they may include a pulsar halo component. We present a pulsar halo model with the Gammapy library for the purpose of assessing halo candidates in Imaging Atmospheric Cherenkov Telescope data, and use it to simulate H.E.S.S. observations of a pulsar halo. We show that the pulsar proper motion can induce the offset typically measured between pulsars and their associated very-high-energy emission.

Keywords: gamma-rays, pulsar wind nebula, pulsar halo

1 Introduction

A gamma-ray pulsar halo is defined as the inverse Compton (IC) emission from escaped electrons and positrons diffusing in the interstellar medium (ISM), injected by a pulsar wind nebula (PWN). The HAWC observatory discovered the halos around PSR J0633+1746 (Geminga) and B0656+14 (Monogem), suggesting that particle diffusion in the halo can be suppressed by 2 to 3 orders of magnitude when compared with the ISM average (Abeysekara et al. 2017). The pulsars surrounded by such halos are generally older ($\gtrsim$ 40 kyr) than those powering PWNe, and the very-high-energy (VHE) and ultra-high-energy (UHE) emission regions can extend to several degrees. Imaging Atmospheric Cherenkov Telescopes (IACTs) are successful in determining the origin of some extended sources, owing to their spatial resolving power. However, the duty cycle and field of view (FOV) of current IACTs limit their ability to search for fainter and/or more extended sources, and direct Extensive Air Shower (EAS) detectors, such as HAWC and LHAASO, are better suited to that end. As such, the analysis of data from IACTs and direct EAS detectors in tandem is a powerful tool, when complementary measurements are available.

LHAASO, with a FOV of 2 steradians and a near full duty cycle, comprises the Water Cherenkov Detector Array (WCDA) which surveys the sky from $\sim$ 0.5 to $\sim$ 30 TeV, and the Kilometer Squared Array (KM2A), which can detect gamma-ray sources above 25 TeV (Cao et al. 2024). Since it began operation, LHAASO has shown that pulsar-powered sources might contribute to the UHE γ-ray sky, such as the case of the Crab PWN (The LHAASO Collaboration et al. 2021). The recently published 1LHAASO catalog (Cao et al. 2024) comprises 90 sources, 43 of which are significant above 100 TeV. We are interested in looking for potential associations of these sources with PWNe. The H.E.S.S. Galactic Plane Survey (HGPS, H.E.S.S. Collaboration et al. 2018a) contains 12 sources firmly identified as PWNe, based on multi-wavelength evidence and/or their energy-dependent morphology, and a further 10 "highly-rated" candidate PWNe (H.E.S.S. Collaboration et al. 2018b, hereafter HESS2018b).

In Section 2, we present the associations between 1LHAASO sources, energetic pulsars and their associated HGPS source. Since some of these sources could potentially be pulsar halos, in Section 3 we develop a spectro-morphological model of a pulsar halo within the Gammapy library (Donath et al. 2023; Acero et al. 2024) in order to search for such objects in IACT data.

[1] Laboratoire Univers et Particules de Montpellier, Université de Montpellier, CNRS/IN2P3, Place Eugène Bataillon, 34095 Montpellier Cedex 5, France

2 Associations between 1LHAASO sources, energetic pulsars and HGPS sources

We considered pulsars in the ATNF pulsar catalog* v1.70 (Manchester et al. 2005) with $\frac{\dot{E}}{d^2} \geq 10^{34}$ erg s^{-1} pc^{-2}, and an age younger than 10^4 kyr, following HESS2018b. There are 68 such pulsars in the region covered by the 1LHAASO survey. We considered the KM2A source components reported in the 1LHAASO catalog. For a given KM2A-detected source, we searched for pulsars within 1.5 times the reported symmetric 2D Gaussian 1σ extension. For point-like sources, we used the reported 95% confidence interval upper limits on the extension. We found that a total of 42 KM2A sources (including 26 which are significant above 100 TeV) are spatially coincident with at least 1 energetic pulsar (7 of them are spatially coincident with 2 pulsars, 2 of them are spatially coincident with 3 pulsars, and one of them is spatially coincident with 5 pulsars). Among these associations, we were particularly interested in those associated with an HGPS source. In the region overlapped by both the HGPS and the 1LHAASO survey ($|b| \leq 3°$ and $\ell \approx 10°$ to $65°$), we found 22 KM2A sources associated with energetic pulsars (including 15 significant above 100 TeV), 10 of which are associated with a pulsar which is in turn associated with a firmly identified or with a highly rated candidate PWN according to HESS2018b (Table 1). Six such associations show a smooth spectral transition from the VHE to the UHE domain when comparing the reported spectral models in the HGPS and 1LHAASO (see Fig. 1 for an example). Of the 6, 5 of these are significant above 100 TeV (marked with "u" in the 1LHAASO catalog). This is an indication that these KM2A sources are the UHE counterpart of the H.E.S.S. sources, and likely have the same origin.

1LHAASO	PSR	HESS	Spectral/Position compatibility	Spin-down age (kyr)
J1809−1918u	J1809−1917	J1809−193	Yes/Yes	54.1
J1814−1719u*	J1813−1749	J1813−178†	Yes/Yes	5.6
J1814−1636u	J1813−1749	J1813−178†	No/No	5.6
J1825−1418	B1823−13	J1825−137†	Yes/Yes	21.4
J1825−1337u	B1823−13	J1825−137†	Yes/No	21.4
J1831−1028	J1833−1034	J1833−105†	No/No	4.9
J1837−0654u	J1838−0655	J1837−069†	Yes/Yes	22.7
J1848−0001u	J1849−0001	J1849−000†	Yes/Yes	43.1
J1852+0050u*	J1849−0001	J1849−000†	No/No	43.1
J1908+0615u	J1907+0602	J1908+063	Yes/Yes	19.5

Table 1: KM2A sources associated with energetic pulsars and H.E.S.S. firmly identified (†) or highly rated candidate PWNe. If a KM2A source is associated with more than one pulsar, the pulsar shown in the table is the one associated to a H.E.S.S. firmly identified or highly-rated candidate PWN (HESS2018b).

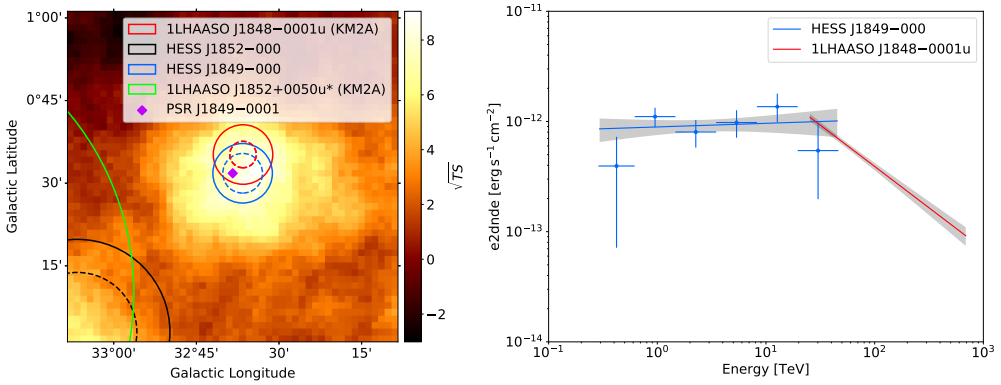

Fig. 1: **Left:** HGPS significance map (TS = Test Statistic) at the position of PSR J1849-0001 overlaid with H.E.S.S. and KM2A sources. The solid lines show the source extension, the dashed lines indicate the 95% confidence interval position uncertainty. **Right:** Reported spectral models of sources associated with PSR J1849-000. The grey regions indicate the 1σ statistical uncertainty range.

*https://www.atnf.csiro.au/research/pulsar/psrcat/

3 Using a pulsar halo model with the Gammapy library

In order to test for a potential presence of a pulsar halo in the sources reported in Table 1, and in IACT data in general, we developed a pulsar halo model with the Gammapy library. We adopt the definition proposed by Giacinti et al. (2020), in which the middle-aged pulsar has exited the parent supernova remnant, possibly forming a bow-shock PWN from which particles can easily escape into the ISM. Thus, particles are continuously injected from a PWN of negligible size compared to the extent of the halo. Our model is similar to the work in H.E.S.S. Collaboration et al. (2023) (see also Tang & Piran 2019; Di Mauro et al. 2019; Martin et al. 2022; Schroer et al. 2023, and references therein): the particle transport is completely diffusive and particles lose energy through IC scattering and synchrotron emission in a uniform ISM magnetic field. The cooling rate from IC scattering, including the Klein-Nishina regime, is computed following Delahaye et al. (2010). We use the spectral energy densities from Popescu et al. (2017) at the pulsar location for the target radiation fields. The diffusion coefficient follows a power law $D(E) = D_0 \left(\frac{E}{E_0}\right)^{\delta}$ and we define the diffusion length scale λ as

$$\lambda^2(E, E') = 4 \int_E^{E'} \frac{D(E'')}{b(E'')}\, dE''$$

where b is the particle cooling rate, E is the present particle energy, E' is the particle injection energy, $E_0 = 100$ TeV is the reference energy, and we set $\delta = \frac{1}{3}$ (Kolmogorov turbulence). The model takes into account the pulsar proper motion, similarly to Di Mauro et al. (2019) and Zhang et al. (2021). As shown in Fig. 2, where we computed the model with the pulsar properties of PSR J1809−1917, the VHE morphology of the pulsar halo is strongly dependent on the diffusion coefficient normalization, the synchrotron cooling rate and the pulsar proper motion.

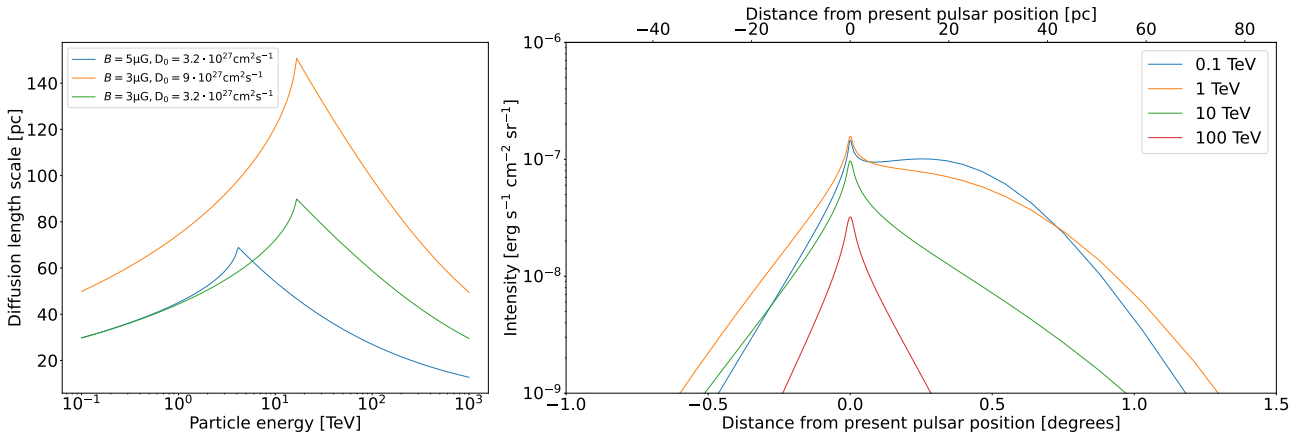

Fig. 2: **Left:** Diffusion radius as a function of particle energy for different model setups. **Right:** Pulsar halo intensity profile at different energies, with the pulsar proper motion taken into account ($V_{PSR} = 500$ km s^{-1}, $D_0 = 3.2 \cdot 10^{27}$ cm^2 s^{-1}, $B = 3$ μG, and the pulsar distance is 3.3 kpc).

The Gammapy python library allows handling of multidimensional models for the analyses of astrophysical sources, and supports the simulation of binned events from observations of a model source. We used the pulsar halo model with the pulsar properties of PSR J1809−1917. Over a grid of the model variables, we computed normalized spatial templates for each photon energy, and the space-integrated gamma-ray spectra. The spatial templates are in units of sr^{-1} and are computed by dividing the pulsar halo intensity profile at each energy (Fig.2) by the value of the total gamma-ray spectrum at said energy. We simulated 86.6 hours of observations of a pulsar halo using the instrument response functions from the observations towards MSH 15−52, which are available in the first public H.E.S.S. data release[†]. We created a 3D events cube and injected Poisson fluctuations. A 2D Gaussian source model with a power law gamma-ray spectrum can then be optimized through likelihood fitting against the simulated data. In the example shown in Fig. 3, we fitted the 2D Gaussian

[†]This work made use of data from the H.E.S.S. DL3 public test data release 1 (HESS DL3 DR1, H.E.S.S. collaboration, 2018). `https://www.mpi-hd.mpg.de/hfm/HESS/pages/dl3-dr1/`

model for simulated observations of a pulsar halo with different pulsar transverse velocities, showing that the latter can induce a significant offset from the pulsar position, similar to the PWNe in HESS2018b, where the offset between HESS J1809−193 and PSR J1809−1917 is reported as ≤ 17 pc.

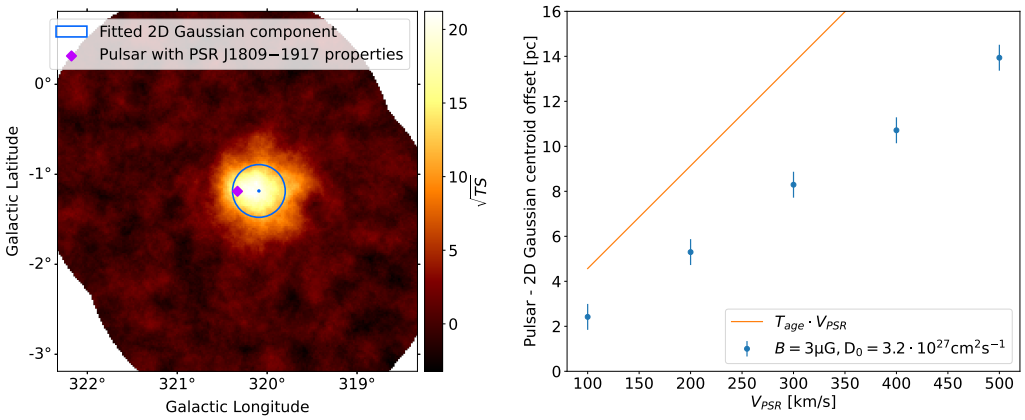

Fig. 3: **Left:** Significance map (from 0.53 TeV to 80 TeV) from simulated observations of a pulsar halo with the same parameters as Fig. 2 (right), overlaid with the best-fit 2D Gaussian component. **Right:** Best-fit 2D Gaussian centroid offset from the pulsar position for simulated observations of a pulsar halo with different pulsar transverse velocities. The yellow line shows the distance travelled by the pulsar during its true age $T_{age} = 44.7$ kyr assuming an initial spin-down period of 30 ms and a braking index of 3.

4 Conclusions

We searched for associations between KM2A components and the pulsars associated with the firmly identified and highly rated candidate PWNe in HGPS data. We identified 6 KM2A counterparts of such H.E.S.S. sources, which have compatible spectra and positions, indicating that the VHE and UHE emission likely has the same origin. We developed a pulsar halo model within the Gammapy library, and to check its validity we used publicly available H.E.S.S. data to simulate observations of a pulsar halo. This model is aimed to be used to identify pulsar halos in H.E.S.S. data and to constrain their properties, and can also be used in any data analysis based in Gammapy.

References

Abeysekara, A. U., Albert, A., Alfaro, R., et al. 2017, Science, 358, 911
Acero, F., Bernete, J., Biederbeck, N., et al. 2024, https://doi.org/10.5281/zenodo.10726484
Cao, Z., Aharonian, F., An, Q., et al. 2024, The Astrophysical Journal Supplement Series, 271, 25
Delahaye, T., Lavalle, J., Lineros, R., Donato, F., & Fornengo, N. 2010, A&A, 524, A51
Di Mauro, M., Manconi, S., & Donato, F. 2019, Phys. Rev. D, 100, 123015
Donath, A., Terrier, R., Remy, Q., et al. 2023, A&A, 678, A157
Giacinti, G., Mitchell, A. M. W., López-Coto, R., et al. 2020, A&A, 636, A113
H.E.S.S. Collaboration, Abdalla, H., Abramowski, A., & et al., A. 2018a, A&A, 612, A1
H.E.S.S. Collaboration, Abdalla, H., Abramowski, A., & et al., A. 2018b, A&A, 612, A2
H.E.S.S. Collaboration, Aharonian, F., Ait Benkhali, F., et al. 2023, A&A, 673, A148
Manchester, R. N., Hobbs, G. B., Teoh, A., & Hobbs, M. 2005, The Astronomical Journal, 129, 1993
Martin, P., Marcowith, A., & Tibaldo, L. 2022, A&A, 665, A132
Popescu, C. C., Yang, R., Tuffs, R. J., et al. 2017, Monthly Notices of the Royal Astronomical Society, 470, 2539
Schroer, B., Evoli, C., & Blasi, P. 2023, Phys. Rev. D, 107, 123020
Tang, X. & Piran, T. 2019, Monthly Notices of the Royal Astronomical Society, 484, 3491
The LHAASO Collaboration, Cao, Z., Aharonian, F., et al. 2021, Science, 373, 425
Zhang, Y., Liu, R.-Y., Chen, S. Z., & Wang, X.-Y. 2021, The Astrophysical Journal, 922, 130